3.3

QUANTIFICATION OF INCREASED STORM SURGE RISK TO PROPERTY AS SEA LEVEL RISES

Ross N. Hoffman,*
Atmospheric and Environmental Research, Inc., Lexington, MA

Peter Dailey,
AIR Worldwide Corp., Boston, MA

Susanna Hopsch, Rui M. Ponte, Katherine Quinn,
Atmospheric and Environmental Research, Inc., Lexington, MA

and Emma M. Hill
Harvard-Smithsonian Center for Astrophysics, Cambridge, MA

January 19, 2010

1. INTRODUCTION

Sea level is projected to continue to rise. Even small differences in sea level have significant impacts on storm surge risk to life and property. Projecting losses to property in the future as sea level rises is made difficult by several factors that result in uncertainty in the future inventory of real estate along the coast. As a first step, we quantify the change in expected risk if sea level were higher *now* by an amount equivalent to a conservative projection of sea level rise over twenty years. Upper and lower bounds of this projection are also evaluated. We then apply a state-of-the-science catastrophe model to quantify the risk of storm surge to coastal property.

Factors that would increase uncertainty, but which are absent in our analysis, include trends in construction practices and regulations that in turn impact property vulnerability, and changes in economic values and population densities. Here the focus is directly on property loss, rather than insured loss, for the current real estate inventory. This eliminates the need to project changing exposure which depends on underwriting trends as well as changes in property values. In addition to sea level rise, many other geophysical factors that may affect storm surge risk, which in turn will have financial impacts, will change with changing climate, such as changes to hurricane characteristics and changes to coastal geometry and ecosystems.

*Corresponding author: Ross N. Hoffman, Atmospheric and Environmental Research, Inc., 131 Hartwell Avenue, Lexington, MA 02421. e-mail: ross.n.hoffman@aer.com

2. MODELING SEA LEVEL RISE

Sea level variations, as measured by tide gauges, are analyzed to project sea level rise in the future along the U.S. Gulf and East Coasts. These rates are extrapolated for twenty years and spatially interpolated to provide a projected increase in sea level in the year 2030 (Fig. 1).

The variation of sea level at a location (as measured by a tide gauge) is caused by numerous processes, which include:

- **Long-term absolute global sea level rise** due to additions of mass, changes in ocean basin volume, and water density changes;
- **Relative local vertical land motions** due to glacial isostatic adjustment, tectonic uplift or subsidence, sediment loading, and extraction of oil, gas, and water;
- **Ocean circulation variability**, which tends to be balanced geostrophically by the mass field;

- **Synoptic weather**, especially storm surge associated with tropical and extratropical cyclones; and
- **Tides** the most predictable component of sea level variability.

Two estimates of long-term sea level change are used here. Both are based on monthly average tide gauge data in which tidal signals on periods less than a day have been filtered out. The first estimate is determined by a simple linear least squares fit to the NOAA tide gauge data (NOAA 2007). These estimates are referred to as the "NOAA model" estimates here. The analysis by NOAA included 67 tide gauges along the U.S. Gulf and East Coasts, all with records of at least 30 years and some with much longer records. These estimates were used to prepare Fig. 1. In what follows we actually subtract these gridded values from the current topography used in the storm surge model described below.

The second estimate is based on the analysis of Hill et al. (2007). The tide gauge data in this case are from the Permanent Service for Mean Sea Level (PSMSL) and cover a period of approximately 40 years. Hill et al. (2007) present several models that explain the variability in the data. The estimates used here are based on what we will refer to as as the "full model" and include accounting for the inverted barometer effect (Ponte 2006), the seasonal cycle, and ocean circulation, as estimated from a dynamical model. The difference in sea level rise between the two methods is coherent along the East Coast with mostly smaller sea level rises north of approximately Washington, DC and larger sea level rises to the south in the full model (Fig. 2).

Hill et al. (2007) used a global selection of high-quality tide gauges that had nearly complete 40-year records. The locations of the NOAA and full model tide gauges in key regions along the East and Gulf Coasts are shown in Fig. 3. Clearly some of the differences seen in Fig. 2 are due to the tide gauges used. Note in particular the two gauges present only in the NOAA model at Eugene Island, Louisiana south of Lake Charles and Sabine Pass, Texas at the Louisiana-Texas border. The red and blue symbols do not exactly overlap because the number of digits recording latitude and longitude were different in the two data sets.

Both sea level models provide an uncertainty estimate for the rate of sea level rise. Generally, at gauges where the ocean variability is significant and not a simple linear trend, the uncertainty of the full model will be less than the uncertainty of the NOAA model. Similarly, where the historical tide gauge record is significantly longer than the 40 years (used by Hill et al. 2007), the NOAA model uncertainty will be less. Overall the uncertainty estimates are similar. In terms of risk uncertainty, the two estimates yield essentially the same results except in North Carolina and the mid-Atlantic region, and to a lesser extent in the Gulf (see Fig. 5 below). To evaluate this uncertainty of our risk impact estimates, we use upper and lower bound (UB and LB) scenarios. For each gauge we replace the model estimate with the 95% confidence interval UB or LB, construct the estimate of sea level rise at 2030 based on these values, and apply the surge model. However, we note that this confidence interval is probably smaller than a true 95% confidence interval because we are simply applying linear regression on past observations to estimate the time rate of change of sea level.

There are some notable geographical variations evident in Fig. 1. In the sections that follow we will explore some of the factors that result in these variations and the impacts of these variations in different regions. In general, low-lying built-up areas are most vulnerable—Florida provides a good example of how storm surge can run up large distances over such areas. In other regions, low elevation combines with other factors to result in greater risk sensitivity. We will examine two such regions below. First, the largest sea level rise occurs along the coast of Louisiana. In this region, sea level rise is enhanced due to a combination of sediment loading, subsidence due to oil and gas extraction, and erosion. Another region of enhanced sea level rise is found on the East Coast, peaking at Chesapeake Bay, where the forebulge at the edge of the icesheet formed during the last glaciation is still relaxing back to pre-glacial equilibrium.

3. MODELING SURGE LOSSES

The surge component of the AIR hurricane catastrophe (CAT) model (hereafter simply the surge model) is used to estimate the change in risk associated with sea level rise. The surge model is a parametric, time-evolving storm surge simulator based on a number of key storm parameters (Fig. 4). The storm parameters are taken from a catalog of 10,000 years of simulated Atlantic tropical cyclones provided by a stochastic hurricane model. The surge model also takes into account several local factors including the bathymetry of the basin (accounting for steep or shallow seafloor off the shore is important for wave build-up), the coastal geometry (*e.g.*, surge amplification in bays), the phase of the astronomical tide, the land elevation, and the terrain roughness (the latter affects how fast waves are attenuated).

Losses are calculated for each year in the catalog. The average annual loss (AAL) is then determined. The AAL is an expectation, *i.e.*, the aggregated losses that can be expected to occur per year when averaged over many years. The distribution of losses also allows us to estimate exceedance probabilities. For example, the 100-year loss corresponds to the level of simulated loss from a single event that has a 1% probability of occurring or being exceeded in any year.

The stochastic hurricane model is based on several empirically determined probability distributions. As a result, the statistics of the simulated storms captures the natural variability of the historical storms, including the space, time, frequency, and intensity characteristics. There are approximately 19,000 landfalling hurricanes in the catalog used here.

The peak surge height is interpolated to the location of each property in the property data base. A civil engineering "vulnerability" model then determines the fraction of the total property value that is damaged as a function of surge height. These parameterizations or "damage functions" are specified for each construction type. Losses to individual properties are then aggregated over zip codes, states, and regions by storm and by year. These are called "ground up" losses.

4. PROJECTED CHANGES IN LOSSES

We compare results from calculating ground up loss according to several scenarios. The Baseline Scenario includes current sea level and the Standard Catalog of 10,000 years of stochastically simulated hurricanes. The NOAA Scenario uses the NOAA model estimate of sea level for 2030, while the Full Scenario includes the full model estimate. Two additional scenarios, denoted Full + WSST and NOAA + WSST, replace the Standard Catalog with the warm sea surface temperature (WSST) Catalog of 10,000 years of stochastically simulated hurricanes. For each scenario, except for the Baseline Scenario, we also calculated losses that correspond to the 95% confidence interval UB and LB estimates of sea level rise.

Aggregate losses for the entire U.S. Gulf and East Coasts (hereafter denoted US when describing losses to the entire region) are displayed in Table 1 for the Baseline, NOAA, and NOAA + WSST Scenarios. Results for the Full and Full + WSST Scenarios, not shown here, are similar. The table shows the AAL, the 50-year return period loss (50 yr RP), and the 100-year return period loss (100 yr RP). Since we do not predict future property values, the relative variations are most meaningful for comparison with future scenarios. Here and in what follows we normalize all dollar amounts by the AAL for the US Baseline Scenario. We define this value to be 1 USBS. For the Baseline Scenario, the AAL is thus 1 USBS, once in 50 years the expected loss will exceed 6.23 USBS, and once in 100 years the expected loss will exceed 7.50 USBS. For the NOAA Scenario, the AAL is 1.08 USBS, an increase of 7.8% relative to Baseline, while for the NOAA + WSST Scenario, the AAL is 1.19 USBS, an increase of 19% relative to Baseline. For the more extreme events, the percentage increases in risk are smaller, *e.g.*, less than half (3% vs. 8%) for the 100-year return period loss under the NOAA Scenario. We will discuss geographic variations of expected loss and changes in loss below.

Table 1: Total aggregate losses (in USBS, *i.e.*, all dollar amounts are normalized by the AAL for the US Baseline Scenario), and as a percent difference from Baseline for the NOAA and NOAA + WSST Scenarios for the entire U.S. Gulf and East Coasts (US). Total aggregate US losses for the Baseline (BL) Scenario are listed for comparison. Losses are given for the aggregate annual average loss (AAL), the 50-year return period loss (50 yr RP), and the 100-year return period loss (100 yr RP).

Type	Units	BL	NOAA	NOAA + WSST
AAL	USBS	1.00	1.08	1.19
	%		7.8	19
50 yr RP	USBS	6.23	6.49	6.66
	%		4.2	6.9
100 yr RP	USBS	7.50	7.73	7.81
	%		3.0	4.1

Figure 5 depicts the uncertainty in the projections of AAL and 50- and 100-year return period losses for the US and for other regions and a number of states. The regions dividing the US are the Gulf (Texas, Louisiana, Mississippi, Alabama), Florida (FL), the Southeast (SE; Georgia, South Carolina, North Carolina), the mid-Atlantic (m-A; Virginia, Delaware, Maryland, Pennsylvania), and the Northeast (NE; New Jersey, New York, Connecticut, Rhode Island, Massachusetts, New Hampshire, Vermont, Maine). For each region or state and for each of the three loss statistics we plot the range of the 95% confidence interval. In the upper panel the range is normalized by the NOAA or Full estimate, while in the lower panel it is normalized by the loss difference, the NOAA or Full estimate minus the Baseline estimate. In the upper panel we see that uncertainty as a percent of our estimates is typically

2-4% except 4-8% for the NOAA Scenarios for the mid-Atlantic region and North Carolina. Further uncertainty does not depend very much on which of the two storm catalogs are used. In the lower panel, uncertainty as a percent of the difference of our estimates from the Baseline are typically 20% except 40-50% for Florida for the Standard Catalog (and therefore for the entire US) as well as for the NOAA Scenario for the Standard Catalog for the mid-Atlantic region and North Carolina.

We now examine how surge risk is expected to vary locally in 2030. In the remainder of this section we will show only results from the Standard Catalog. Figure 6 shows the current estimate of ground up loss cost for the Baseline Scenario. Ground up loss cost is a measure of fractional loss, *i.e.*, dollars of AAL per thousand dollars of property value. Ground up loss cost due to storm surge is very large along the Louisiana coast, large in southwest Florida, and substantial along much of the coast of Florida, Georgia, and North Carolina, in the Delaware Bay, and in some locations in Texas. In the following we will focus on three regions that are particularly vulnerable due to different combinations of factors affecting sea level rise. We will highlight variations in our risk estimates due to differences between the NOAA and Hill *et al.* projections of sea level rise.

a. *Low-lying land in Florida*

When storm surge overtops natural and man-made coastal defenses, low-lying land substantial distances inland can be at risk. Vulnerability to sea level changes has greatly increased due to coastal development, often on very low-lying areas such as barrier islands, in the U.S. and especially in Florida during the last several decades. The states with the largest areas of low-lying land are Louisiana (with 24,725 square kilometers of land at risk between 0 and 1.5 meters and 4,345 square kilometers between 1.5 and 3.5 meters), Florida (with 12,251 and 12,743 square kilometers at risk), North Carolina (with 5836 and 3865 square kilometers at risk), and Texas (with 5178 and 4213 square kilometers at risk) (Titus and Richman 2001). We will return to Louisiana and North Carolina shortly, but first consider the case of Florida. Figure 7 shows the areas below 1.5 m (red) and between 1.5 and 3 m above sea level (blue). Clearly enormous areas of South Florida are at risk, but note also that much of the West Coast of Florida has large areas at or below 3.5 m. As a result most of the Florida coastline is vulnerable to hurricane storm surge. Areas at greatest proportional risk are on the south Gulf Coast of Florida, notably from Fort Myers southwards towards Cape Sable (Fig. 6).

In Fig. 8 we compare the percentage change in ground up loss cost relative to Baseline along the Florida and Georgia Coasts for NOAA and Full Scenarios. Here, the most noticeable percentage increase occurs at Waccasassa Bay (north of Tampa Bay and south of Apalachee Bay), an area with relatively small Baseline risk. In fact, percentage increases are relatively small in just those areas where the loss cost differences with respect to the Baseline Scenario were greatest. Differences between the NOAA and Full Scenarios appear minor except on the southern shores of Tampa Bay where increases in risk are much larger under the Full Scenario. Values displayed in this figure are normalized by the total value and do not highlight areas where the greatest increases in aggregate losses are expected to occur. Even small rates of risk can aggregate to large values in metropolitan areas such as Miami and Tampa, or in regions of wealth such as the barrier island beaches along the east coast of Florida from Miami northward to Cape Canaveral.

Figure 9 shows the actual (not percentage) difference (NOAA – Full) in projected losses for Florida. Here we see alternating bands of risk difference from south to north with larger risks for the NOAA Scenario in south and north Florida and larger risks for the Full Scenario in the Keys and middle of the state. This pattern mirrors the pattern of Fig. 2.

b. *Land subsidence in Louisiana due to fluid extraction*

The Mississippi delta region of Louisiana is rapidly sinking due to compaction of existing sediments and loading of the crust as new sediments are deposited from river outflow. The coastal areas of Louisiana and Texas are also sinking due to sediment compaction, in large part due to nearby on-shore and offshore oil and gas extraction (Morton et al. 2005). Figure 10 shows that the largest subsidence rates (red colored circles) occur where the transects cross an oil and gas field.

The vulnerability of the Gulf Coast to surge as shown in Fig. 6 is very large from Galveston Bay in Texas all across Louisiana and Mississippi to Biloxi, with some additional "hot" spots south of Galveston. This vulnerability is extreme in the Mississippi Delta area and around Port Arthur, TX. In Fig. 11 we compare the percentage change in ground up loss cost relative to Baseline along the Gulf Coast for NOAA and Full Scenarios. These patterns are similar but percentage increases in expected losses tend to be greater in the NOAA Scenario in Louisiana, particularly southwest of New Orleans near Morgan City and larger in the Full Scenario near Freeport, Texas. Figure 12 shows the actual difference (NOAA – Full) in projected losses for the Gulf. Here we see greater expected losses from Port Arthur, Texas to Terrebonne Parish, Louisiana in the NOAA Scenario and vice versa in most of Texas from Galveston Bay south and in Louisiana from New Orleans to the Delta in the Full Scenario.

c. *Land subsidence in the Carolinas and mid-Atlantic due to post-glacial rebound*

Variations in long-term relative sea level trends along the Northeast Coast are primarily due to different rates of post-glacial rebound from the end of the last ice age when the Laurentide ice sheet melted. Just to the south, in the mid-Atlantic region, the opposite is occurring with land now subsiding at up to 4 $\mathrm{mm\,yr^{-1}}$ that was previously uplifted at the edge of the ice sheet (Calais et al. 2006). These two phenomena are linked by the ongoing reversal of viscous motion of the mantle during the last ice age from the loaded area under the ice cap to the unloaded surrounding areas. This is illustrated in Fig. 13.

The greatest vulnerability to storm surge in this region is centered on Cape Hatteras, from the southern reaches of the Pamlico Sound to Virginia Beach. Additional areas at risk are the eastern shores of the Chesapeake and Delaware Bays. Relatively minor surge risk exists for Atlantic City, NJ and New York Harbor, particularly Jamaica Bay. Of course these qualifiers—“greatest”, “minor”—are for the relative risk in terms of loss cost. The huge property values in New York City mean that actual total risk may be great in a New York zip code with a relatively small loss cost.

In Fig. 14 we compare the percentage change in ground up loss cost relative to Baseline along the North Carolina and mid-Atlantic Coasts for the NOAA and Full Scenarios. In both cases the largest percentage increases are far from the ocean in low-lying areas that currently have low risk, including the upper reaches of the Delaware Bay and along the Pamlico River and Albermarle Sound inland of Cape Hatteras. No significant differences between the two scenarios are apparent.

Figure 15 shows the actual difference (NOAA – Full) in projected losses for the Carolinas and Cheasapeake Bay areas. Along the Carolinas, the Full Scenario projects larger losses. In the interior of the Cheasapeake and Delaware Bays, the NOAA Scenario projects larger losses. Along the Delmarva Peninsula and New Jersey Atlantic Coast we see an alternating pattern of loss differences between the two scenarios.

5. CONCLUDING REMARKS

The storm surge module of the AIR hurricane CAT model is used to estimate the sensitivity of storm surge risk to sea level rise. To accomplish this, land elevations used are reduced from current values by the projected sea level increases at 2030. For each scenario, we calculated property value losses for the current property inventory for 10,000 simulated years of tropical storms, including 19,000 landfalls. Losses due to wind or rain were not included.

The Baseline Scenario results (*i.e.*, for current conditions, as shown in Fig. 6) were compared to the results from two different estimates of sea level rise and two different stochastic hurricane catalogs. Upper and lower bound estimates were calculated in all cases. The estimates of sea level rise are either based on a simple linear regression of all available tide gauge data (NOAA 2007), or based on combining model simulations with tide gauge data over a 40-year period (Hill et al. 2007). These estimates of sea level rise were used in the NOAA and Full Scenarios, respectively. The hurricane catalogs are the Standard and Warm SST (WSST) AIR Catalogs, but we report almost exclusively on results from the Standard Catalog here.

Our sea level rise estimates are conservative since the true sea level rise may be accelerating and this acceleration may increase in the future. For example, Church and White (2006) report improved fits for the global sea level rise by allowing a change in slope or quadratic in time behavior. Part of this change in slope may be related to accelerating ice cap melting. For example, Pfeffer et al. (2008) estimate maximum flow rates for Greenland that correspond to rates of total sea level rise in the range of $8-20$ $\mathrm{mm\ yr^{-1}}$ through the end of the century. These factors would change our estimates of risk as well as increase the uncertainty of our estimates. Even without this effect, we almost certainly underestimate the uncertainty in our projections because our extrapolations neglect variability on decadal and shorter time scales. For example, ocean circulation decadal variability might give faster or slower rates (or even negative rates) of local sea level rise over 10- to 20-year periods.

The calculations described here should be considered a sensitivity study, differing from a realistic projection of loss in several important aspects. We do not include changes to property along the coast (density, value, and construction techniques), changes to coastline due to future erosion and human activities (sea walls, beach replenishment, etc.). Second, a number of studies have tried to determine how tropical cyclone frequency and intensity might vary as climate changes in the future (*e.g.*, Emanuel et al. 2008). Here, however, storm characteristics are held constant to either current conditions or current conditions during years of warm SST (WSST, Dailey et al. 2009). Results of WSST sensitivity experiments will be presented in detail elsewhere (Hoffman et al. 2010).

Principal findings are that:

- Expected losses increase everywhere as sea level rises.

- By 2030, East and Gulf Coast AAL are expected to increase by 8% if tropical storm activity does not change and 19% if tropical storm activity is similar to that of the WSST Catalog.

- Uncertainties in Fig. 5 are typically lower for the full model relative to the NOAA model, suggesting the benefits of removing low frequency variability in the tide gauge records, using methods like those studied by Hill et al. (2007), when estimating sea level trends from relatively short records.

- Areas that already have large dollar losses also have large projected increases in dollar losses, but areas that currently have small losses are projected to see the largest projected *percentage* increases.

While this is a sensitivity study, it does provide an example of downscaling climate projections to quantitative projections of future risk. Simple answers and precise projections are not possible when it comes to projecting the future of the climate system and how ecosystems and society will adapt. But society must still make critical decisions. We believe that studies such as this one can inform decision makers to enable the design of resilient strategies.

Acknowledgments. Tide gauge data used in this study came from the PSMSL and NOAA (NOAA 2007). E. M. Hill was supported by the NASA grant NNX07AM77G.

References

Calais, E., J. Y. Han, C. Demets, and J. M. Nocquer, 2006: Deformation of the North American plate interior from a decade of continuous GPS measurements. *J. Geophys. Res.*, **111 (B06402)**, doi:10.1029/2005JB004 253.

Church, J. A. and N. J. White, 2006: A 20th century acceleration in global sea-level rise. *Geophys. Res. Lett.*, **33 (L01602)**, doi:10.1029/2005GL024 826.

Dailey, P. S., G. Zuba, G. Ljung, I. M. Dima, and J. Guin, 2009: On the relationship between North Atlantic sea surface temperatures and U.S. hurricane landfall risk. *J. Appl. Meteor. Climatol.*, **48 (1)**, 111–129.

Emanuel, K., R. Sundararajan, and J. Williams, 2008: Hurricanes and global warming: Results from downscaling IPCC AR4 simulations. *Bull. Amer. Meteor. Soc.*, **89 (3)**, 347–367.

Hill, E. M., R. M. Ponte, and J. L. Davis, 2007: Dynamic and regression modeling of ocean variability in the tide-gauge record at seasonal and longer periods. *J. Geophys. Res.*, **112 (C05007)**, doi:10.1029/2006JC003 745.

Hoffman, R. N., P. Dailey, S. Hopsch, R. M. Ponte, K. Quinn, and E. M. Hill, 2010: An assessment of increased storm surge risk to property due to sea level rise in the first half of the 21st century. *WCAS*, submitted.

Miller, L. and B. C. Douglas, 2006: On the rate and causes of twentieth century sea-level rise. *Phil. Trans. R. Soc. London*, **A362**, 805–820, doi: 10.1098/rsta.2006.1738.

Morton, R. A., J. C. Bernier, J. A. Barras, and N. F. Ferina, 2005: Rapid subsidence and historical wetland loss in the Mississippi delta plain: Likely causes and future implications. Open-file Report 1216, U. S. Geological Survey, 116 pp.

NOAA, 2007: Linear mean sea level (MSL) trends and 95% confidence intervals in mm/yr. Web site, Center for Operational Oceanographic Products and Services, http://tidesandcurrents.noaa.gov/sltrends/msltrendstable.htm.

Pfeffer, W. T., J. T. Harper, and S. O'Neel, 2008: Kinematic constraints on glacier contributions to 21st-century sea level rise. *Science*, **321**, 1340–1343, doi: 10.1126/science.1159099.

Ponte, R. M., 2006: Low frequency sea level variability and the inverted barometer effect. *J. Atmos. Oceanic Technol.*, **23**, 619–629.

Titus, J. G. and C. Richman, 2001: Maps of lands vulnerable to sea level rise: Modeled elevations along the U.S. Atlantic and Gulf Coasts. *Climate Research*, **18 (3)**, 205–228.

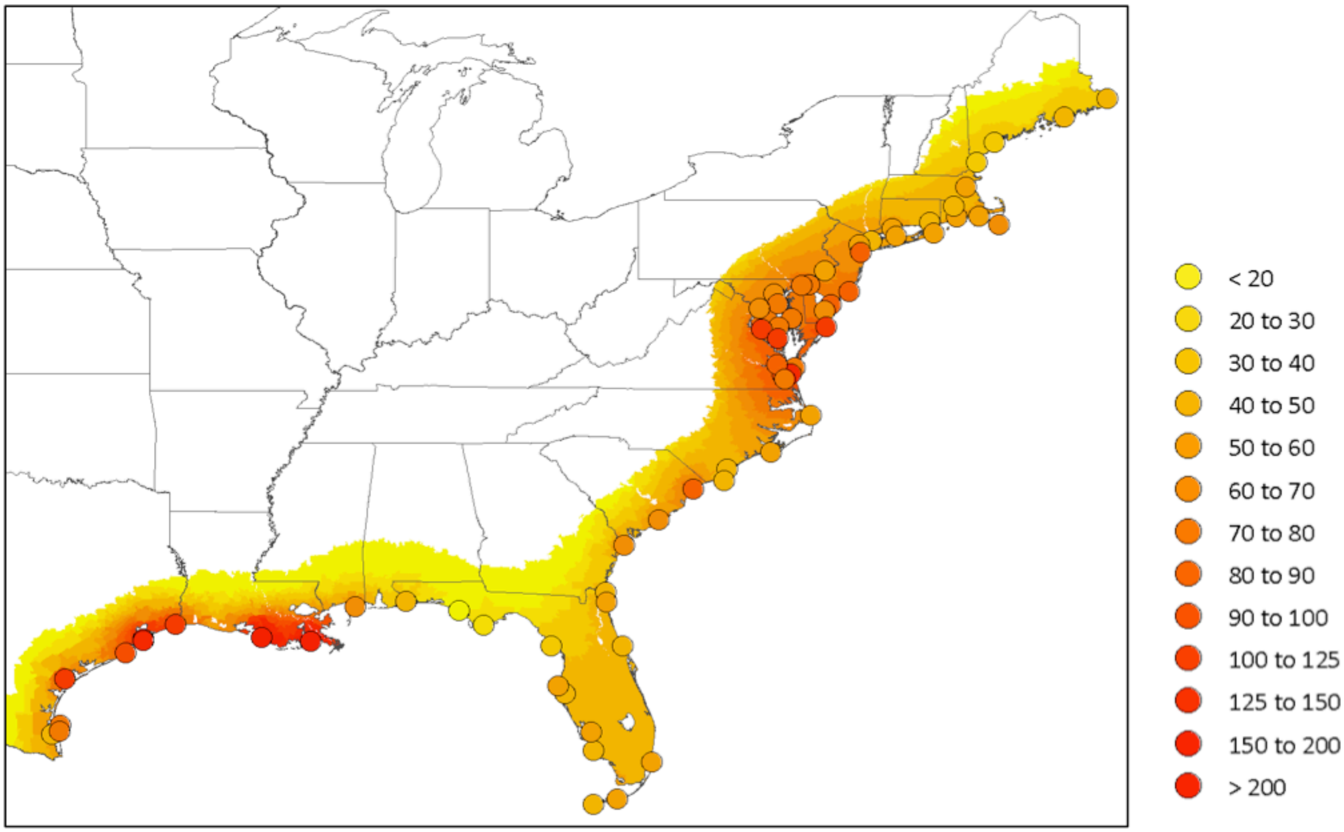

Figure 1. The 2030 projection of sea level rise (mm) based on the NOAA model extrapolation of tide gauge records. Projected increases in sea level are color coded in the circle plotted at each tide gauge location. Gridded values, using the same color scale, were calculated as the weighted average of the tide gauge values, with weights inversely proportional to distance between the grid point and the tide gauge. Gridded values are plotted only in the coastal region approximately 100 miles wide that includes all areas at risk from storm surge.

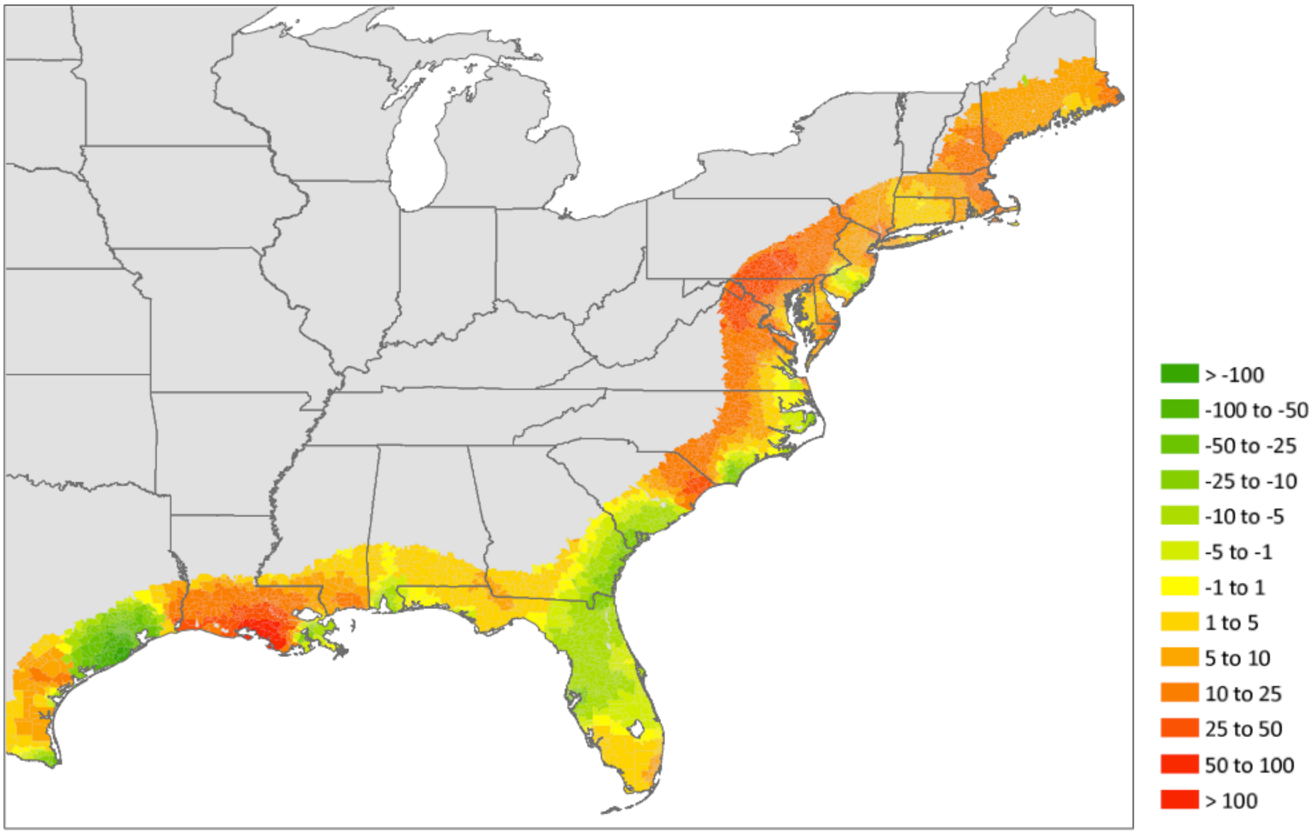

Figure 2. Difference between projected sea level in 2030 for NOAA and full models in mm (NOAA-Full). Red tones indicate that the NOAA Scenario projected elevation adjustment is larger and green tones indicate that the Full Scenario adjustment is larger. Differences are due to both differences in sea level rise estimates and differences in the observation station networks (see Fig. 3).

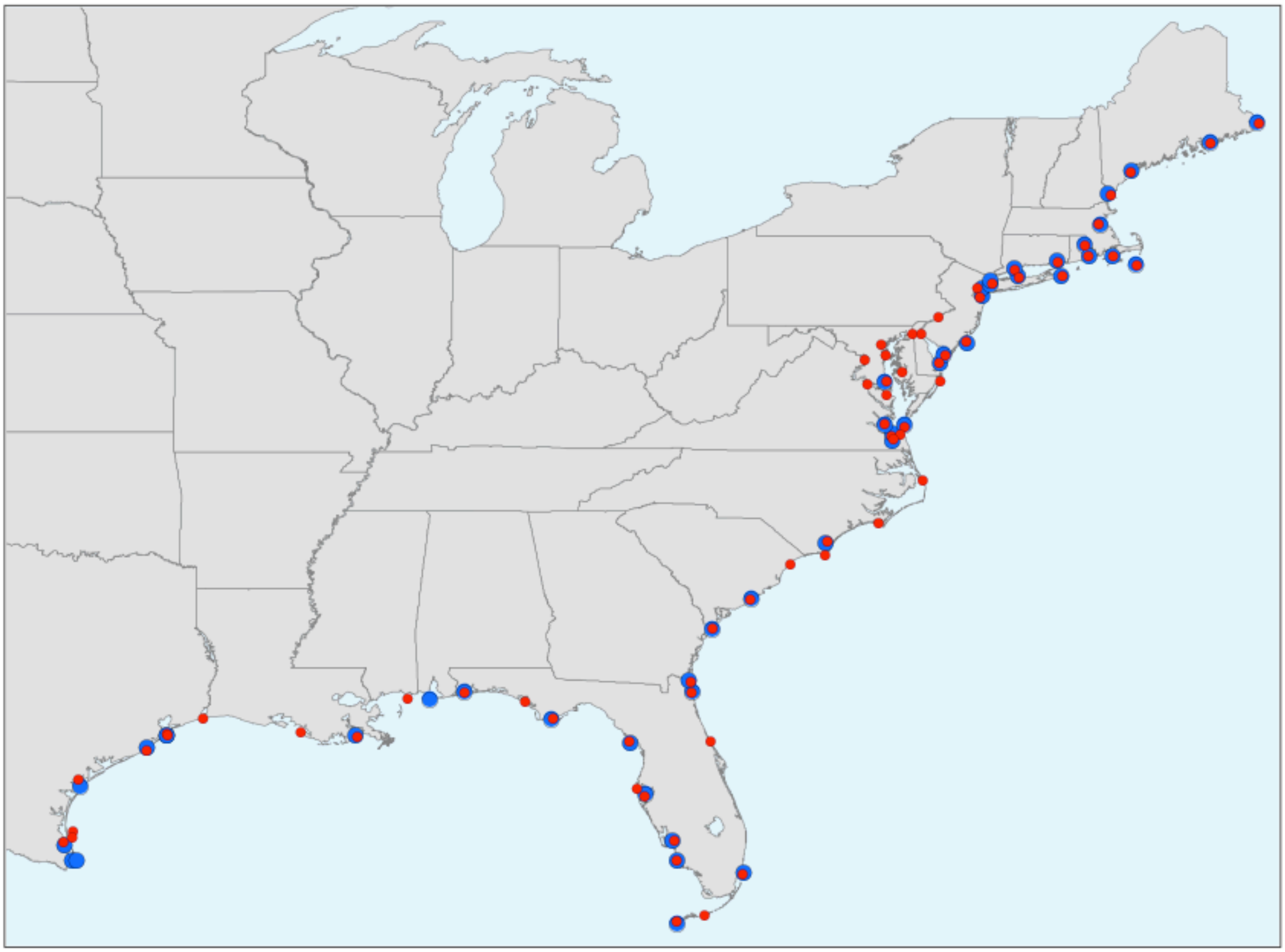

Figure 3. Location of tide gauges used to create the NOAA (red) and Hill et al. (blue) projections. Note that there are regional differences in the station network density between the two data sets, such as in the upper Chesapeake Bay area, Cape Hatteras and Louisiana.

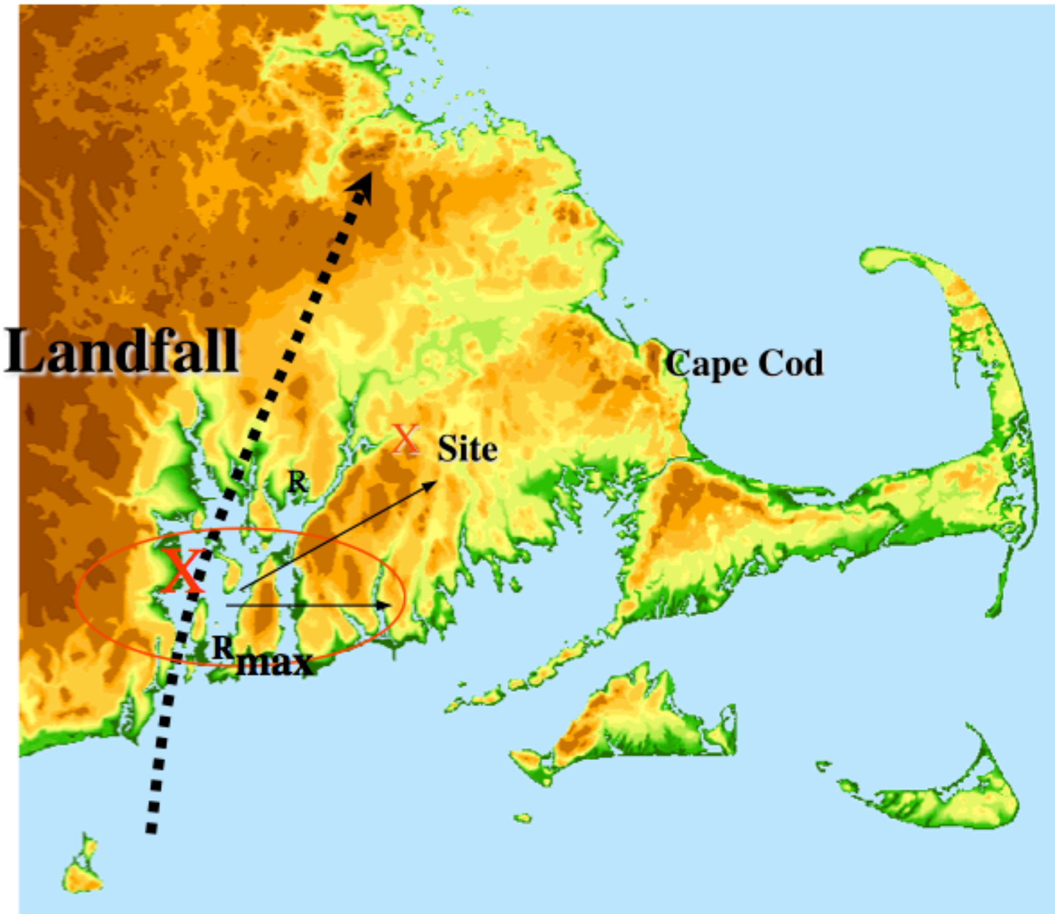

Figure 4. The AIR storm-surge model. Storm parameters include maximum wind speed, central pressure, size (radius of maximum winds), forward speed, and track.

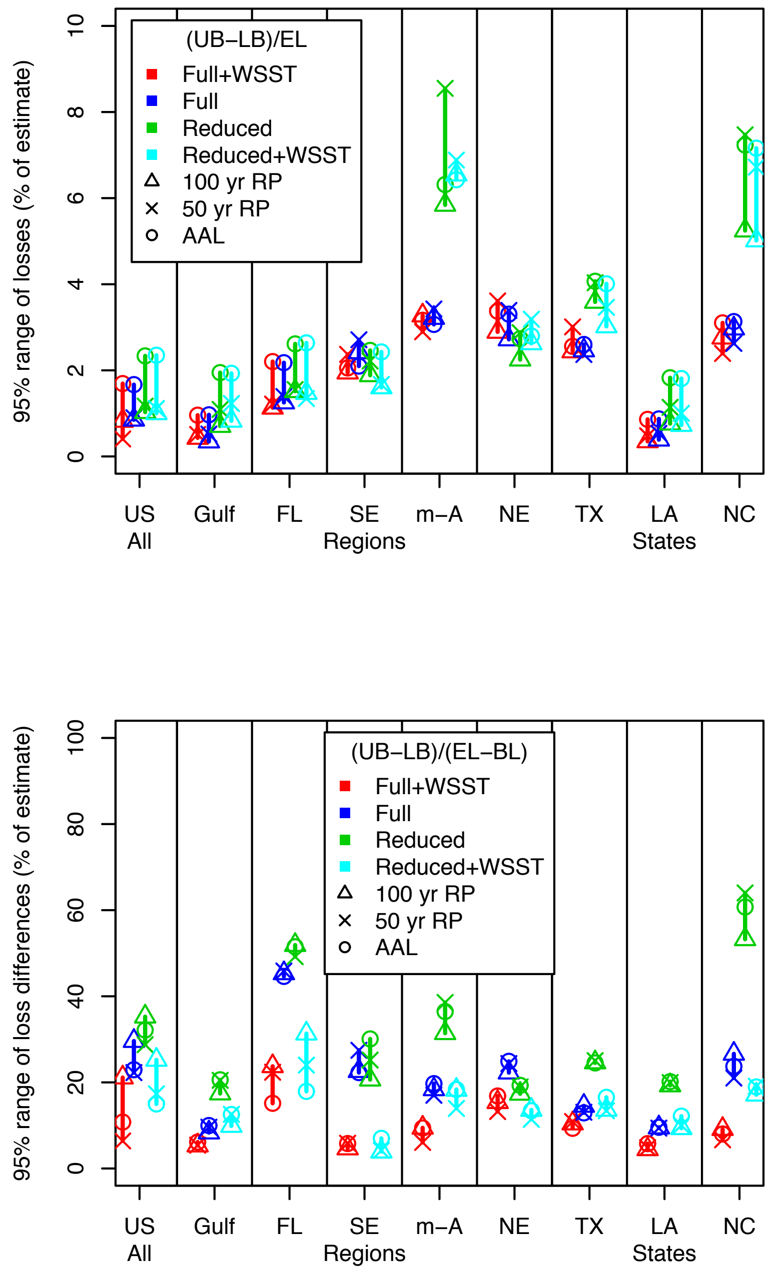

Figure 5. Aggregate loss uncertainties in per cent. A different color is used for each scenario and a different symbol for each loss as indicated in the legend. In the upper panel, each uncertainty (range of the 95% confidence interval) is normalized by the corresponding estimated loss (EL) for that scenario, while in the bottom panel, the uncertainty is normalized by the corresponding estimated increase in loss relative to the baseline. Regions are defined precisely in the text (e.g., m-A indicates mid-Atlantic). NB: This uncertainty is due only to the uncertainty in the estimated slope of sea level rise.

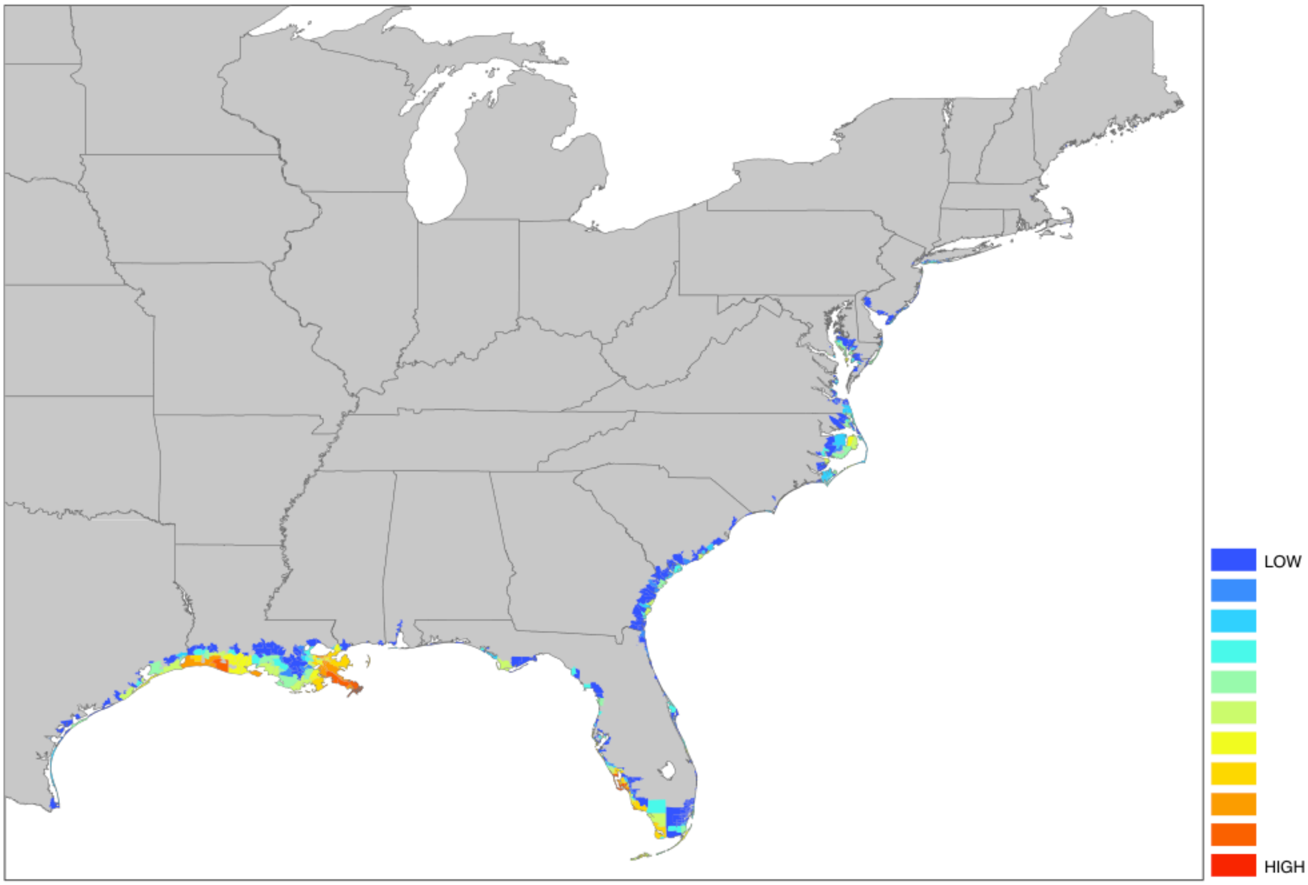

Figure 6. The Baseline Scenario ground up loss cost ($/1000) along the U.S. Gulf and East Coast by zip code. Only losses due to tropical cyclone surge damage are included. The ground up loss cost is the expected annual loss in dollars per thousand dollars of property. Values are based on current sea level using the Standard Catalog of 10,000 years of simulated tropical cyclone. The color scale from deep blue to dark red indicates increasing loss costs on a geometric scale with the maximum value doubling from hue to hue. Numeric values are not given because only the relative variations are meaningful for comparison with future scenarios. Areas with no expected surge losses are light grey.

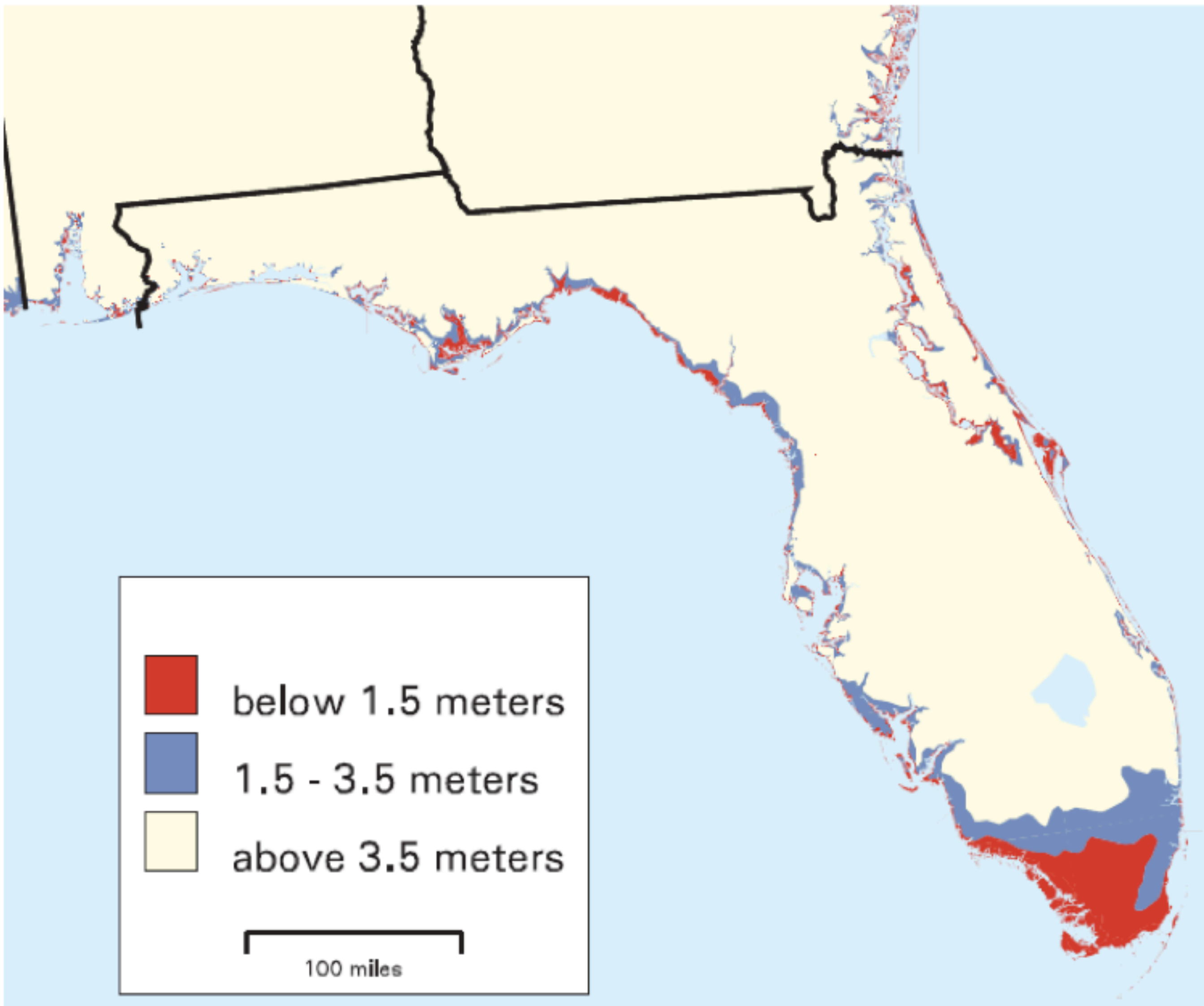

Figure 7. The location and extent of low-lying areas in Florida. (Source: EPA)

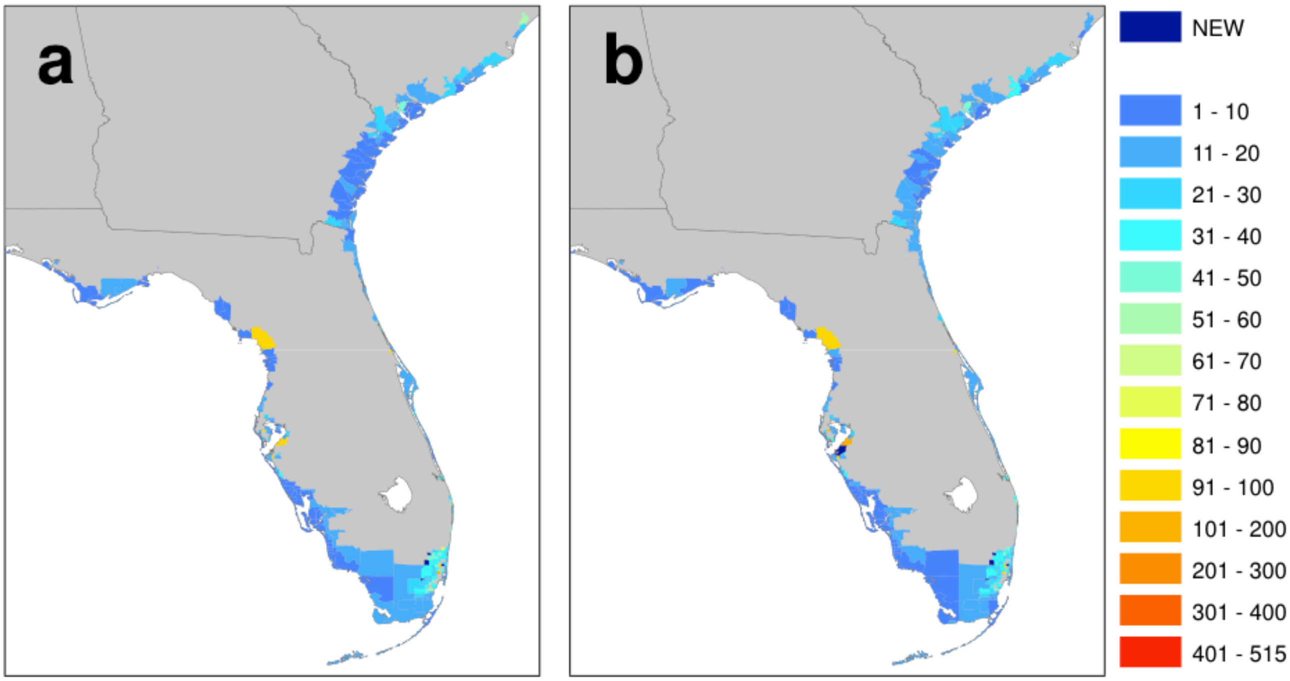

Figure 8. The percentage change in ground up loss cost relative to the Baseline Scenario along the Florida Coast for the (a) NOAA and (b) Full Scenarios. The percentage change is relative to current conditions, i.e., a 100% change corresponds to a doubling of the estimated loss. For the most part, areas showing the largest percentage increases are areas that currently have very small expected surge losses. Areas with no expected surge losses in 2030 are light grey and areas with some expected surge losses in 2030, but none currently, are dark blue (labeled "NEW" in the legend).

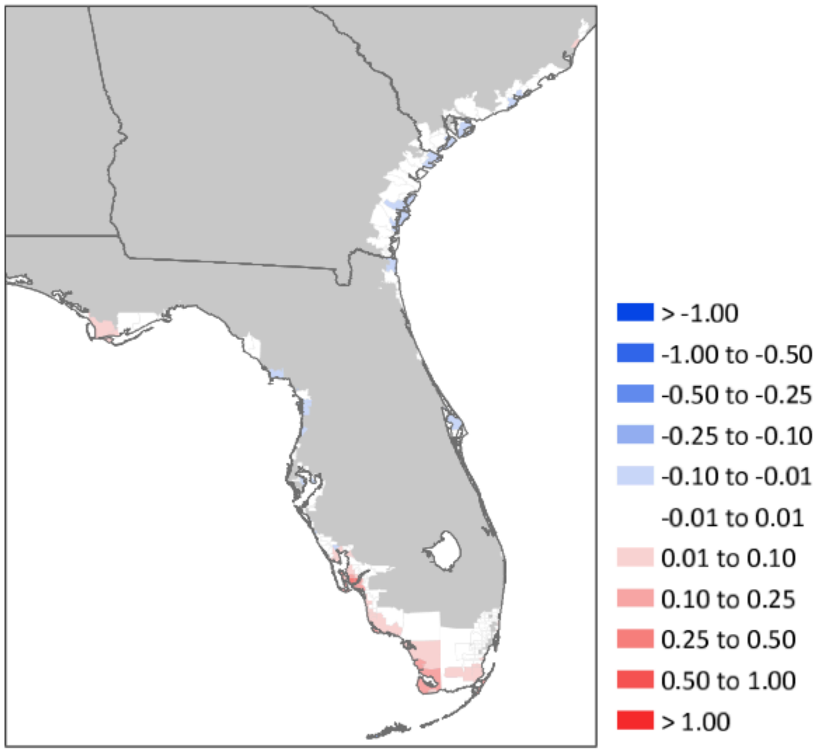

Figure 9. The difference in ground up loss cost between the NOAA and Full Scenarios by zip code (NOAA – Full) for Florida. The color scale from light pink to red indicates increasingly higher loss cost values of the NOAA Scenario relative to the Full Scenario. The light blue to blue color scale in turn indicates increasingly higher loss cost values of the Full Scenario relative to the NOAA Scenario. Areas with no expected surge losses in 2030 are light grey.

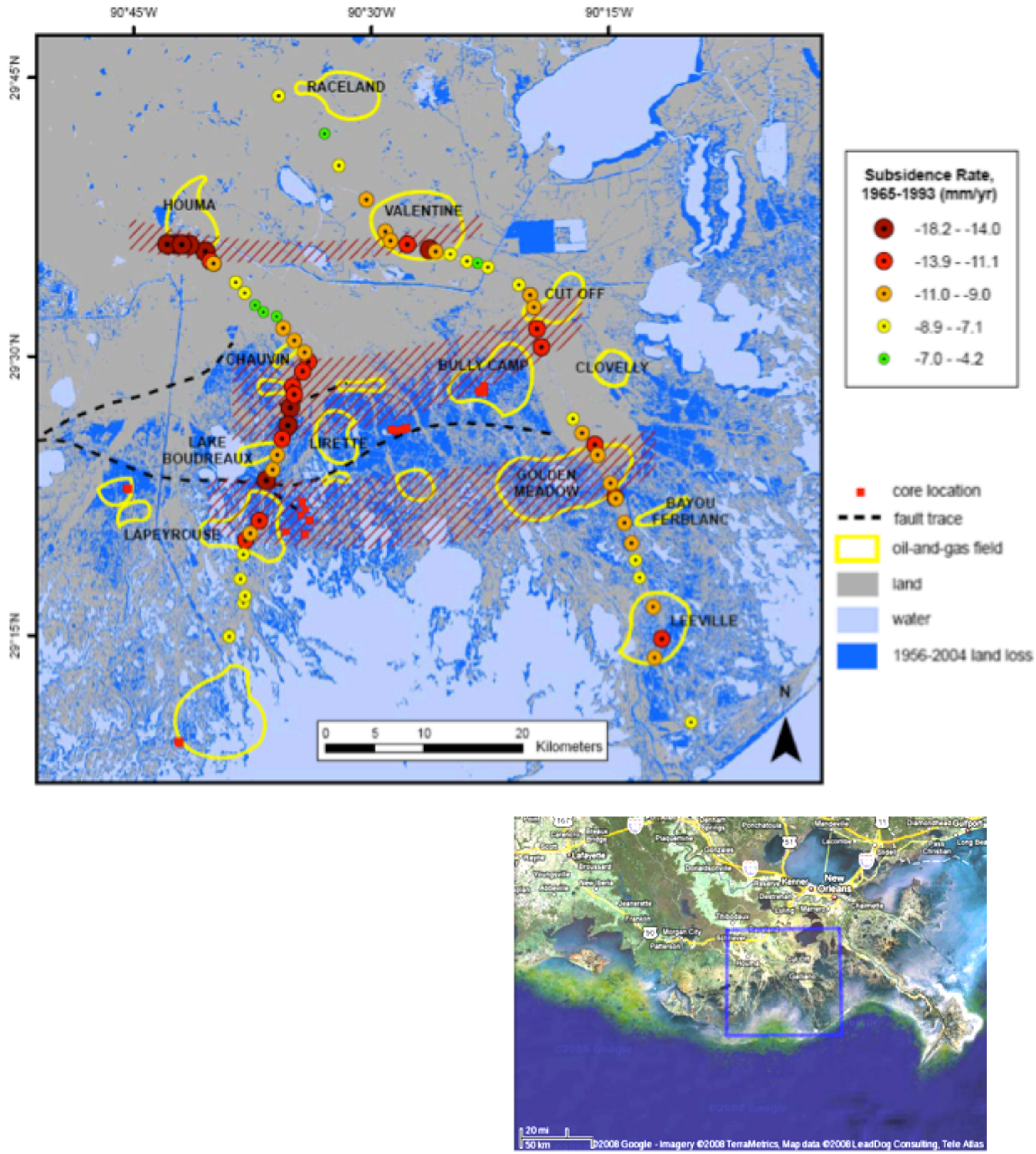

Figure 10. Map of average subsidence rates between 1965 and 1993 in south Louisiana. Subsidence rates calculated by the National Geodetic Survey. Areas of highest average subsidence rates (> 12 mm/yr; hatched pattern) correlate closely with locations of oil-and-gas fields. Lower panel shows the location of the upper panel. (Figure 10 from Morton et al., 2005.)

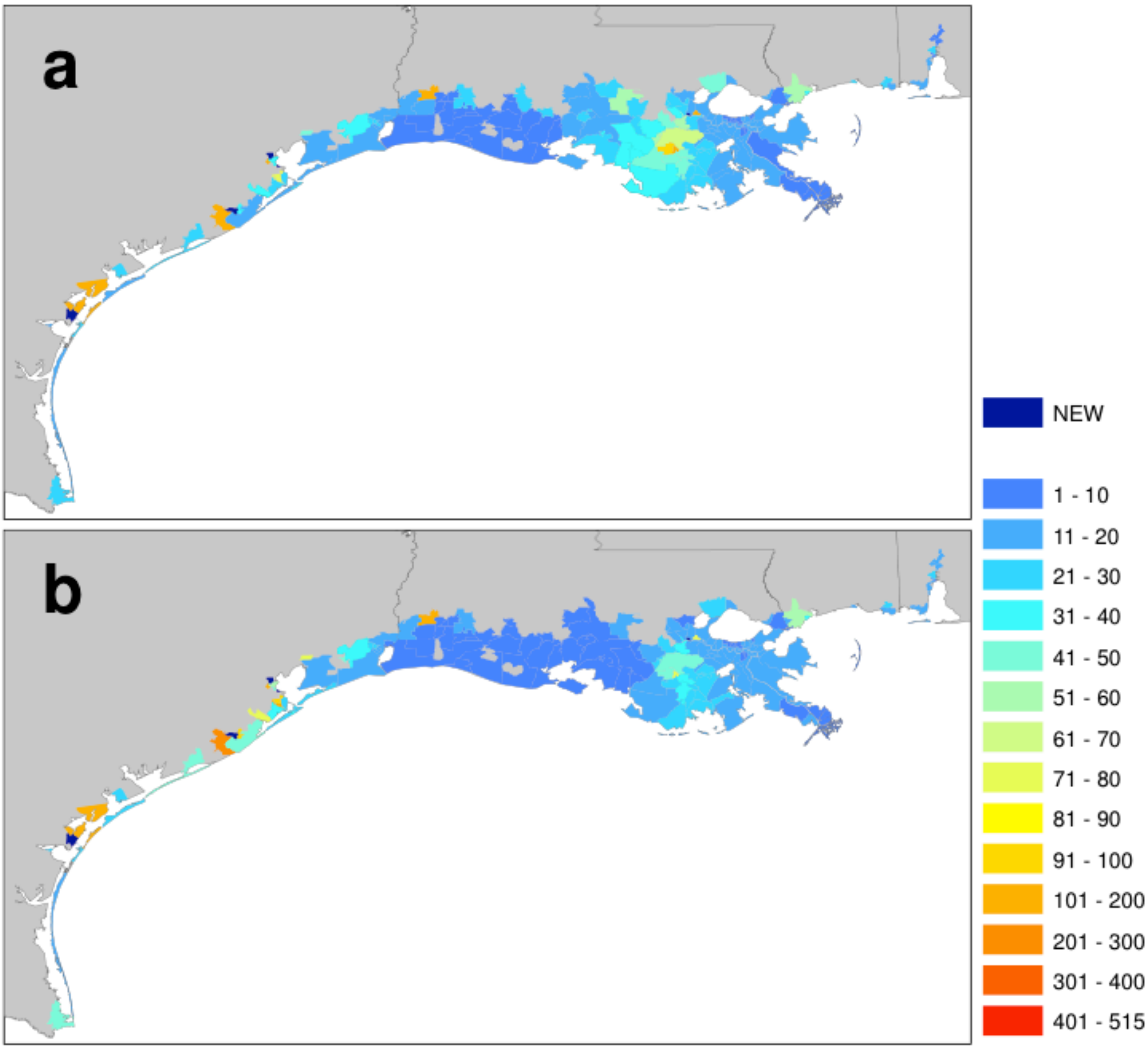

Figure 11. The percentage change in ground up loss cost relative to the Baseline Scenario along the Gulf Coast for the (a) NOAA and (b) Full Scenarios. Plotted as in Fig. 8.

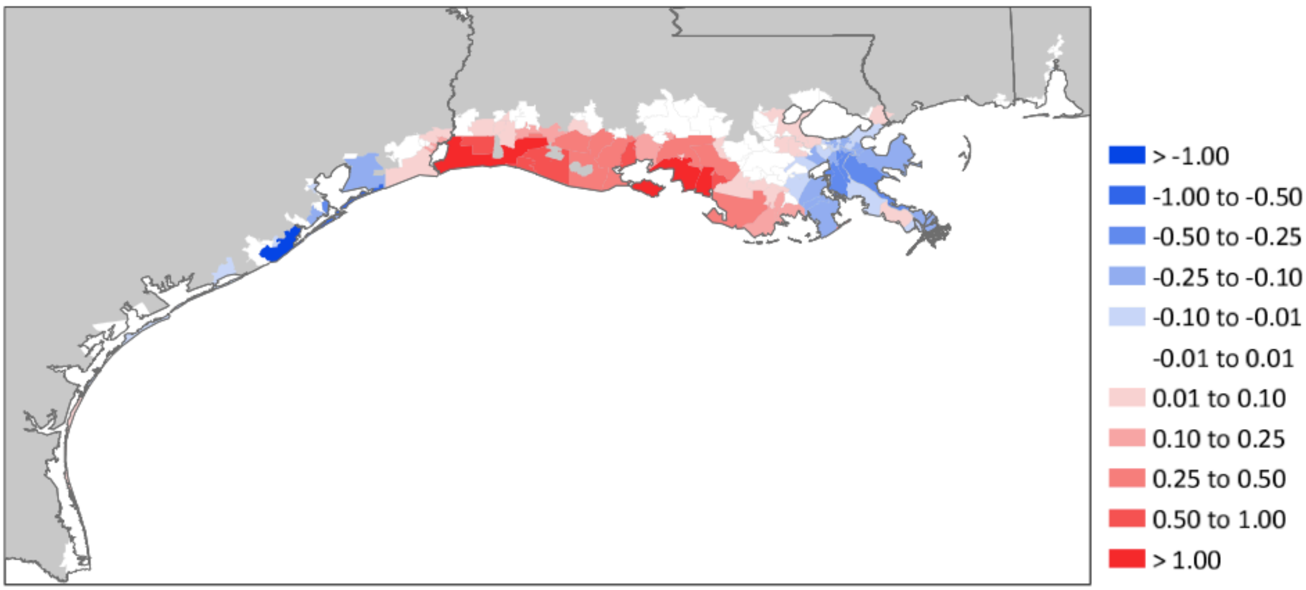

Figure 12. The difference in ground up loss cost between NOAA and Full Scenarios along the Gulf Coast. The differences are due to a combination of different estimates in sea level rise, as well as due to differences in observation network density (see Fig. 3). Plotted as in Fig. 9.

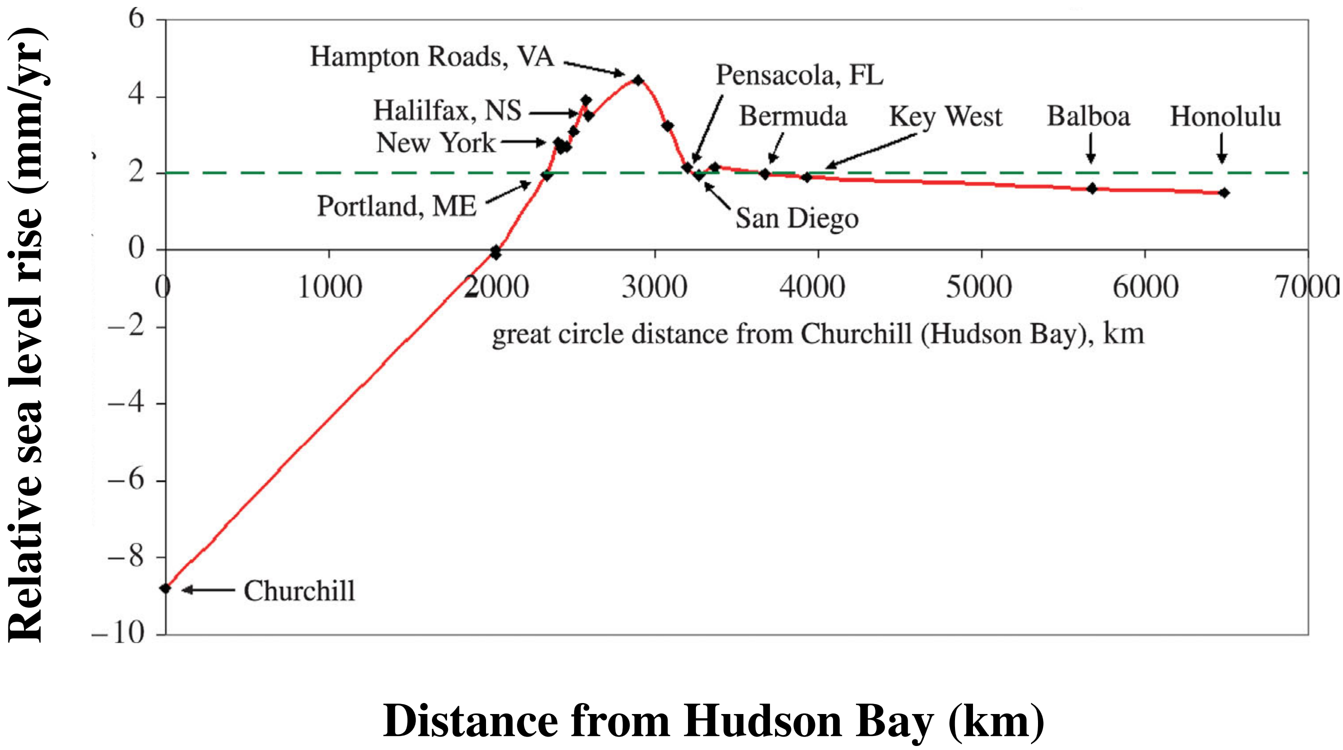

Figure 13. Sea level rise as a function of distance to Churchill, Canada. The collapse of the glacial fore-bulge causes enhanced subsidence along the mid-Atlantic and North Carolina Coasts. To aid visualization, a green dashed line is drawn at 2 mm yr^{-1}. (Fig. 4 of Miller and Douglas, 2006.)

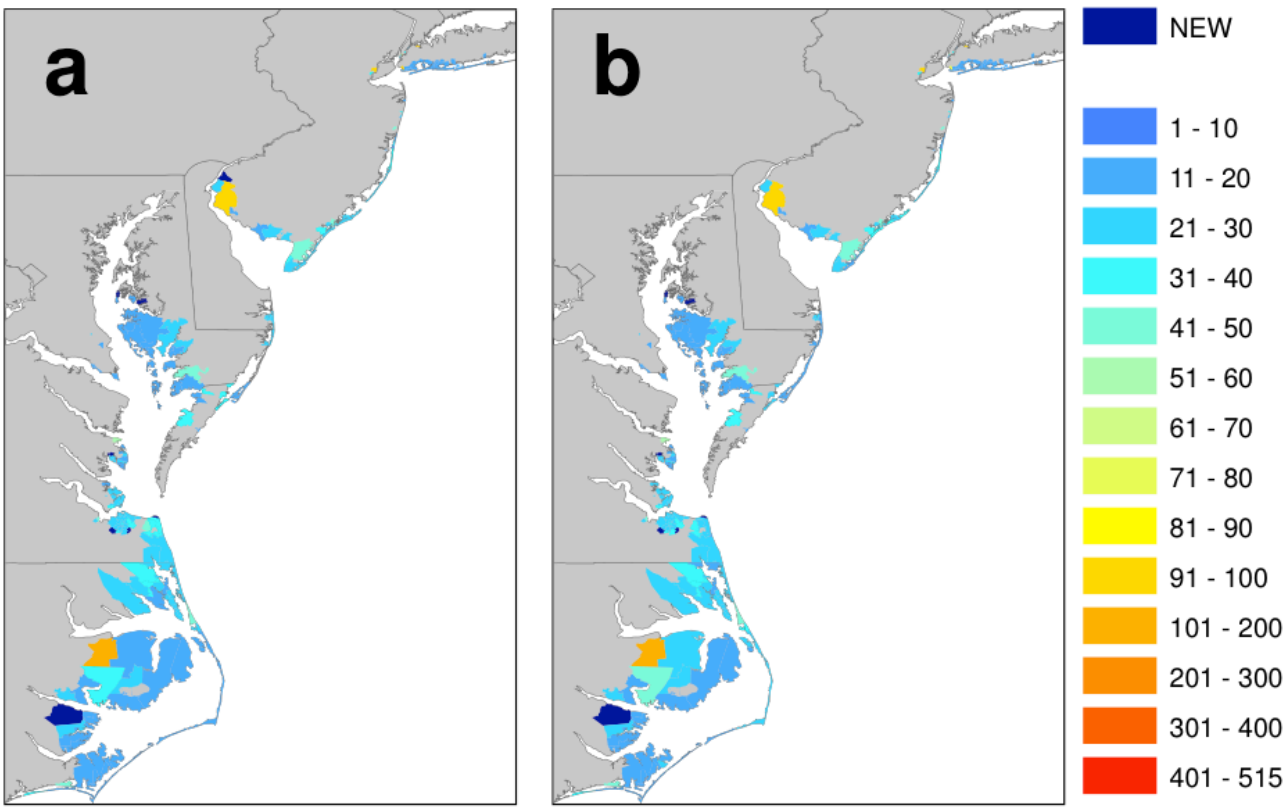

Figure 14. The percentage change in ground up loss cost relative to the Baseline Scenario along the Mid-Atlantic Coast for the (a) NOAA and (b) Full Scenarios. Plotted as in Fig. 8.

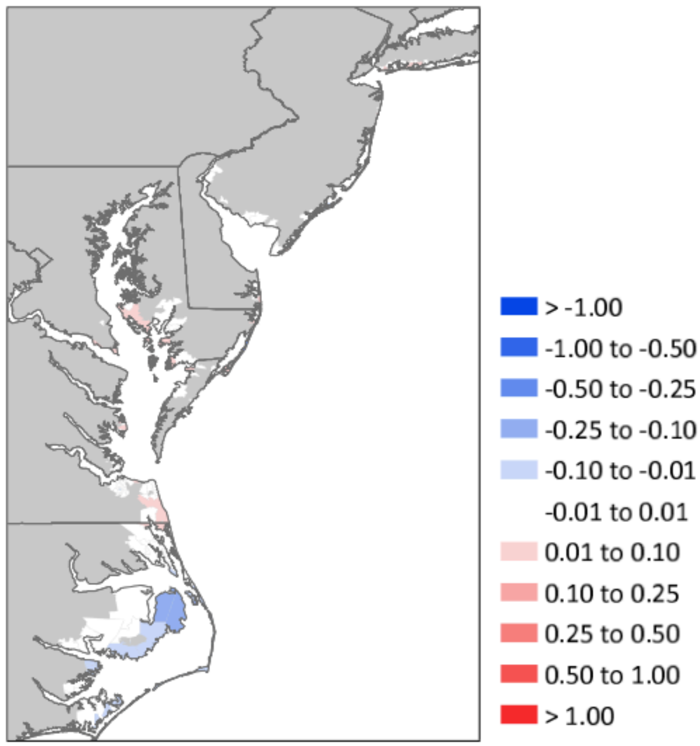

Figure 15. The difference in ground up loss cost between the NOAA and Full Scenarios in the region (top) and along the Carolinas Coast (bottom). Plotted as in Fig. 9.